

13. N. I. Nikolaev, Diffusion in Membranes [in Russian], Moscow (1980).
14. V. V. Ovchinnikov, V. D. Seleznev, V. V. Surguchev, and V. I. Tokmantsev, Preprints of Presentations, International Symposium on Membranes for Gas and Vapor Separation, Suzdal (USSR) (1989), p. 112.

CAPACITY AND ACOUSTIC-EMISSION METHODS OF STUDYING
TURBULENT-CAVITATION FLOWS OF A FLUID IN POROUS
PERMEABLE MATERIALS

Yu. Yu. Belous

UDC 532.621

We present results from an investigation into the hydrodynamic flows of a fluid through porous materials; these investigations involve two developed methods and we have demonstrated their high sensitivity to the appearance of cavitation bubbles.

Porous permeable materials (PPM) are used extensively in liquid filtration and heat exchange in various branches of industry [1], and the forming flows [2] exert predominant influence on the efficiency of these processes. We presently have on hand a developed and tested range of various methods to study liquid flows in channels and these include mechanical [3], acoustic [4], electromagnetic (conductometric) [5], optical [6], and nuclear-physical [7]. However, the areas in which these methods can be employed to investigate the flows of a fluid in the microcapillaries of pores is extremely limited as a consequence of the specific nature of PPM structure. The goal of this study therefore involves the laying of a foundation for and the experimental verification of the capacity and acoustic-emission methods of examining turbulent-cavitation flows in PPM.

We know [8] that microcapillary channels in PPM are a form of a labyrinth with diversely distinct cross sections which are formed by the elements of the structure. The motion of a liquid about the curvilinear surface of the PPM channels is accompanied by deformation of the flow and the onset of turbulence [9], i.e., local fluctuations in velocity, pressure, and temperature; here we also find a reduction in the cavitation strength of the moving liquid [10]. When the local pressure is lower than the vapor saturation pressure, cavitation sets in [11], and this phenomenon is characterized by a pulsating vapor-gas phase which sends out acoustic waves into the surrounding medium. Consequently, having measured the cavitation index D , equal to the ratio of the component gas volumes ΔV_i of the phase in the liquid V_0 [12] and the amplitude-frequency characteristics (AFC) [2], we can qualitatively and quantitatively evaluate the turbulent-cavitation flows. On this basis, to achieve our stated goal, we have developed a PPM model to serve as a sensor, and this is a round disk of a sintered tantalum (niobium) powder. The structure of the formed materials pertains to the class of PPM and serves as an adequate analog of those materials used for filtration, heat exchange (Fig. 1). We know [1] that PPM exhibits large specific wetting areas, and the treatment of the tantalum (niobium) with H_3PO_4 acid forms thin current-insulating films on the material's surface. This makes it possible to come up with a high-capacity capacitor in which one of the plates is a PPM structure, while the current-conducting fluid (electrolyte) serves as the second. The capacitance here depends on the extent to which the PPM structure is completely filled, as well as on the uniformity of the liquid phase. Thus, we can make the assumption that with the onset of cavitation in the investigated PPM with a pore volume of V_0 the forming vapor-gas bubbles ΔV_i alter the initial capacitance C_0 of the capacitor by ΔC_i , and the quantities $V_0 \approx C_0$, $\Delta V_i \approx \Delta C_i$ will be equivalent. Connecting this device (Fig. 2)

Fiftieth October Anniversary Aviation Production Enterprise, Kiev. Translated from *Inzhenerno-Fizicheskii Zhurnal*, Vol. 57, No. 4, pp. 624-627, October, 1989. Original article submitted April 5, 1988.

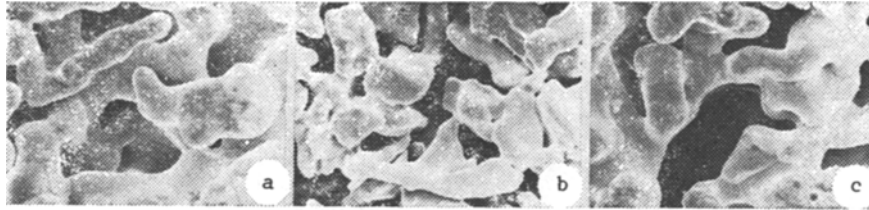


Fig. 1. Porous permeable materials: a) tantalum (niobium); b, c) FNS-5 and PNS-10 filtration materials. 2000 \times .

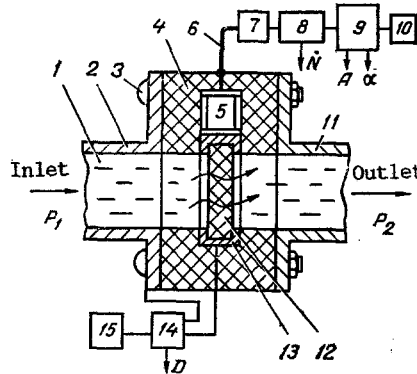


Fig. 2. PPM model sensor device and circuitry of the metering control-recording equipment: 1) aqueous solution of sodium polyphosphate (dielectric fluid); 2, 11) flanged conduits; 3) coupling screws; 4) Teflon inserts; 5) LTZ-19 AE sensor; 6) coaxial cable; 7) signal amplifier; 8) AF-15 acoustic-emission instrumentation; 9) AI-4096A-90 pulse analyzer; 10) DPU digital printout unit; 12) model of porous permeable material, tantalum (niobium); 13) waveguide; 14) TESLA-M capacity meter; 15) K-12-22 loop oscillograph.

to capacitance metering systems and to a loop oscillograph enables us to determine the instantaneous value of ΔC_i and to calculate the cavitation index $D = \Delta C_i / C_0 \approx \Delta V_i / V_0$.

The second assumption is based on the fact that the acoustic waves of turbulent-cavitation flows are propagated through liquids and metals in analogy with [13]. As a consequence of this similarity we can conclude that the acoustic emission (AE) signals in the form of mechanical waves arising and propagating through the materials as their structures undergo local dynamic restructuring are characteristic of turbulent-cavitation flows and are found at the beginning of the megahertz range [14]. We have selected the following parameters to be recorded: \dot{N} , the intensity of the AE signals, indicating the quantity of imploding cavitation bubbles; A , the amplitude of the AE signals, whose square characterizes the energy of the imploding cavitation bubbles; α , the amplitude distribution of the AE signals, which provides information on the quantity of cavitation bubbles imploding with different energies, and which is determined by the expression [15]

$$\alpha = K / \ln \dot{N}_0. \quad (1)$$

The AE signals generated by the turbulent-cavitation flows were received by the tantalum PPM and by means of a lead titanate-zirconate piezoceramic sensor (LTZ-19), these signals were then amplified and separated, to be analyzed by AE equipment [14] (Fig. 2).

The investigation followed a program which included determining the sensitivity of these methods to turbulent-cavitation flows and the establishment of an interconnection between the cavitation indices and the amplitude distribution of the AE signals.

For this purpose, in the first stage, the device (Fig. 2) was filled with a three percent aqueous solution of sodium polyphosphate and its original capacitance was measured. An ultrasonic dispersion vibrator (USDV-2M), positioned near the PPM model, was subsequently employed to generate a cavitation area at frequencies of 22 and 44 kHz, with a power of 0.1 kW. The

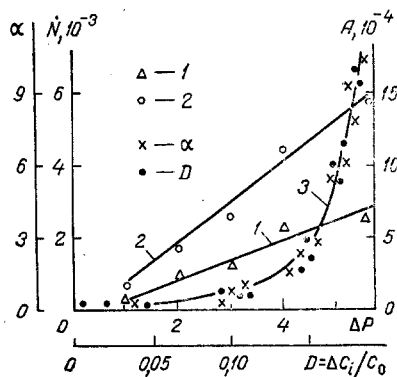


Fig. 3. Results from the measurements of capacity, AE signals, and from the calculation of the amplitude distribution α and the cavitation index D : 1) $\dot{N} = f(\Delta P)$; 2) $A = f(\Delta P)$; 3) $\alpha = f(\Delta P)$ and $\alpha = f(D)$.

\dot{N} , A , ΔC_i parameters were recorded by means of the developed circuit (Fig. 2) and this enabled us to determine the zone of maximum cavitation intensity, which corresponded to the production rating data and confirmed the validity of the assumptions made earlier, demonstrating the high sensitivity of the capacity and AE methods to the turbulent-cavitation properties of the liquid.

The investigations continued with the pumping of the same solution through the PPM model, with a change in the pressure drop ΔP equal to the ratio of the pressures P_1 and $P_2 = 0.1$ MPa. It follows the derived results (Fig. 3) that an increase in ΔP above unity leads to the appearance of AE signals which are stochastic in nature. This can be explained by the onset of the formation of detachment processes within the pore channels of the PPM and the appearance of microcavitation events [11]. A further change in ΔP leads to a stable increase in the \dot{N} and A signals, which may be approximated by straight lines. Calculation and analysis of D and α (Fig. 3) showed that there exists between them a correlation relationship with a probability no worse than $\mathcal{P} \geq 0.7$ and here, with an increase in $\Delta P \geq 4$, we observe a significant growth of α , which gives evidence of the intensification of the turbulent-cavitation flows which are displaced into the region of higher energies. The flowrate characteristic of the PPM [1] is impaired, i.e., the large increase in ΔP corresponds to small increments in the rate of liquid flow through the structure. In this connection it may be concluded that each PPM structure exhibits a critical value for the amplitude distribution of the AE signals, limited by the cavitation index.

Thus the experiments which we have carried out and the derived results enable us to draw the following conclusions: the AE signals \dot{N} and A provide information on the quantity and amplitude of the pulsation cavitation regions; the amplitude distribution of the AE signals is equivalent to the cavitation number of flows for both the current carrying and dielectric fluids in the PPM. We should take note of the fact that the transition to dielectric fluids calls for a particular approach and is achieved after calibration of the entire system by means of a current-conducting aqueous solution, with particular attention being devoted in this case to the stability of the combined constriction of the waveguide and the PPM model in the device. This makes it possible to obtain minimum changes in the wave constants of the device and provides for excellent reproducibility of the research results.

The methods developed here are extremely sensitive to the turbulent-cavitation phenomena and make it possible to generate fluid flow regimes through porous permeable materials in a number of technological processes such as filtration, heat exchange, etc.

NOTATION

D , cavitation index; ΔV_i , gas-phase volume of cavitation region; V_0 , initial fluid volume (the volume of pores in the porous permeable material); C_0 , initial capacitance of the tantalum (niobium) sensor, i.e., the model of the porous permeable material; ΔC_i , the increment in capacitance as a consequence of the formation of a cavitation gas phase; \dot{N} , intensity of the acoustic-emission signals; A , amplitude of the acoustic emission signal; α , amplitude distribution of the acoustic emission signals; K , width of the window in which the AE pulses are recorded; \dot{N}_0 , maximum number of pulses in the initial channel; P_1 , P_2 , pressure in front of and behind the barrier made of the porous permeable materials; $\Delta P = P_1/P_2$, pressure difference across the porous permeable material barrier.

LITERATURE CITED

1. S. V. Belov, P. A. Vityaz', V. K. Sheleg, et al., Porous Permeable Materials [in Russian], Moscow (1987).
2. A. G. Reynolds, Turbulent Flows in Engineering Applications [Russian translation], Moscow (1979).
3. V. V. Vasinger, Atom. Ener., 29, Issue 3, 202-203 (1970).
4. V. I. Mel'nikov and G. B. Usygin, Acoustic Diagnostic Methods for Two-Phase Coolants in Nuclear Power Plants [in Russian], Moscow (1987).
5. A. V. Marchenko, B. P. Golubev, and E. P. Svistunov, Teploénergetika, No. 7, 58-61 (1979).
6. V. S. Sukhorukikh, Contemporary Experimental Methods of Investigating the Processes of Heat and Mass Exchange [in Russian], Minsk (1981), pp. 124-130.
7. M. I. Rezinkov and Z. L. Miropol'skii, Radioisotope Methods of Studying Processes within Boilers [in Russian], Moscow (1964).
8. V. M. Kaptsevich, V. K. Sheleg, A. I. Sorokina, et al., Poroshk. Met., No. 3, 57-59 (1987).
9. L. G. Loitsyanskii, The Mechanics of Liquids and Gases [in Russian], Moscow (1973).
10. É. S. Arzumanov, Cavitation in Local Hydraulic Resistances [in Russian], Moscow (1979).
11. V. V. Rozhdestvenskii, Cavitation [in Russian], Leningrad (1977).
12. L. D. Rozenberg, Powerful Ultrasonic Fields [in Russian], Moscow (1968), pp. 221-266.
13. V. A. Shutilov, The Fundamentals of Ultrasonic Physics [in Russian], Leningrad (1980).
14. V. A. Greshnikov and Yu. B. Drobot, Acoustic Emission [in Russian], Moscow (1976).
15. I. G. Nosovskii, N. G. Stadnichenko, and I. A. Zhigalov, Resp. Mezhved. Nauch.-Tekh. Sb., Issue 28, 43-46, Kiev (1985).

A GENERALIZED EQUATION FOR THE TEMPERATURE CURVE OF THE PROCESS OF CONVECTIVE DRYING OF MOIST MATERIALS

P. S. Kuts, A. I. Ol'shanskii, and V. Ya. Shklyar

UDC 001.57:685.31.001.5

We present the derivation and analysis of the generalized equation for the temperature curve describing the process of drying in continuously operating convective drying installations with a nozzle-directed stream. The results from the numerical solution are compared against experimental data.

A generalized equation has been derived in [1] which describes the kinetics of the process involved in the convective heating of moist materials and which links the kinetic characteristics of the process with the properties of the material and of the heat carrier, as well as with the geometry of the drying installation, and the temperature and hydrodynamic conditions under which the drying process occurs.

The heat-balance equation for the period of a declining rate of drying has the form

$$\bar{\alpha}(T_m - T_s)F = rm_0 \left| \frac{d\bar{u}}{d\tau} \right| + (c_0 m_0 + c_{mo} \bar{m}_{mo}) \frac{d\bar{T}}{d\tau} \quad (1)$$

or

$$\bar{St}(T_m - T_s)F = \frac{1}{c_p \rho v} \left[rm_0 \left| \frac{d\bar{u}}{d\tau} \right| + (c_0 m_0 + c_{mo} \bar{m}_{mo}) \frac{d\bar{T}}{d\tau} \right], \quad (2)$$

A. V. Lykov Institute of Heat and Mass Exchange, Academy of Sciences of the Belorussian SSR, Minsk. Translated from Inzhenerno-Fizicheskii Zhurnal, Vol. 57, No. 4, pp. 627-631, October, 1989. Original article submitted May 13, 1988.